Preparation and Some Properties of Stereocomplex-Type Poly(lactic acid)/Layered Silicate Nanocomposites

Yukiko Furuhashi,[1,*] Kousuke Morioka,[1,2] Hideyuki Tamegai,[2] Naoko Yoshie[1]

[1]International Research Center for Sustainable Materials, Institute of Industrial Science, The University of Tokyo, Meguro-Ku, Tokyo 153-8505, Japan
[2]Department of Chemistry, College of Humanities and Sciences, Nihon University, Setagaya-ku, Tokyo 156-8550, Japan
*Present address: R&D Center, Tokyo Electric Power Company, 4-1 Egasaki-cho, Tsurumi-ku, Yokohama 230-8510, Japan
Correspondence to: N. Yoshie (E-mail: yoshie@iis.u-tokyo.ac.jp)

ABSTRACT: Stereocomplex-type poly(lactic acid)- [PLA]- based blends were prepared by solution casting of equimolar PLLA/PDLA with different amounts of organo-modified montmorillonite. The homocrystallization and stereocomplexation of PLAs were enhanced by annealing of the blends. The stereocomplexation of PLAs, intercalation of the polymer chains between the silicates layers, and morphological structure of the filled PLAs were analyzed by wide-angle X-ray diffraction and transmission electron microscope. Thermogravimetric analyses (TGA), differential scanning calorimetry (DSC), and tensile test were performed to study the thermal and mechanical properties of the blends. The homo- and stereocomplex crystallization of neat PLLA/PDLA were enhanced by annealing. The effect of annealing on the crystallization was emphasized by the addition of clay. With this structural change, thermal stabilities properties were also improved by the addition of clay. The silicate layers of the clay were slightly stacked but intercalated and distributed in the PLA-matrix. © 2012 Wiley Periodicals, Inc. J. Appl. Polym. Sci. 000: 000–000, 2012

INTRODUCTION

Poly(lactic acid), PLA, which can be produced from primary resources like corns, sugars, or beets, is considered to be one of the most promising environmentally friendly materials.[1] Although PLA has a fairly high melting temperature in comparison with other biodegradable polyesters, its T_m around 180°C, is not high enough for some applications. One of the fundamental techniques to enhance thermal stability of PLA is to produce so called "stereocomplex-type crystal" in the equimolar blend of poly(L-lactic acid), PLLA and poly(D-lactic acid), PDLA. This stereocomplex crystal melts at a temperature about 50°C higher than T_m of the homocrystal of PLLA and PDLA. There are many reports on the stereocomplexation of PLA, showing formation mechanism, morphology, and degradation behavior.[2–23] Since the homocrystallization is kinetically favored within the case of high molecular weight PLAs, the stereocomplex crystallization of PLA only occurs under limited conditions. One of the present authors reported that annealing of a drawn fiber of PLLA/PDLA blend above T_m of the homocrystal gave a fiber consisting mainly of stereocomplex crystal.[24,25] We have also developed a simple preparation method for stereocomplex-
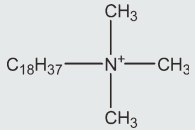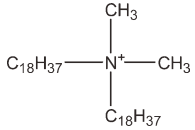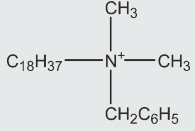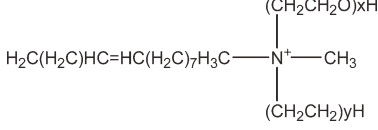
type PLA films, recently.[26] When an equimolar mixture of PLLA and PDLA is cast from mixtures of solvent and nonsolvent of PLA, the PLA films with very high stereocomplex crystallinities can be obtained.

To improve practical utilities such as heat resistance, impact resistance, processability, and flame retardancy of PLLA while maintaining its environmental sustainability, the effect of bio-based additives has been studied. Heat resistance and mechanical strength of PLLA is improved by reinforcing it with modified kenaf[27] and cellulose spun fibers.[28] Composites consisting of PLLA and calcium phosphate particles such shows large surface fracture energy.[29]

Polymer/layered silicate nanocomposites have also been the focus of academic and industrial attention in recent years because the composites often exhibit desired enhancement of physical and chemical properties relative to the neat polymer matrix even at very low clay contents.[30] Layered silicate is naturally abundant, economical, and more importantly, benign to the environment. Recently, there have been several reports on the fabrication of PLLA/layered silicate nanocomposites.[31–39] The increases in tensile strength, modulus, and elongation were observed.

Table I. Characteristics of Organoclays

Clay type	Content of inorganic component/%	Basal spacing/nm	Chemical structure of organic modifier
TM (trimethylstearyl ammonium)	25.6	1.96	$C_{18}H_{37}$—N^+(—CH_3)(—CH_3)—CH_3
DO (dimethyloctadecyl ammonium)	41.8	3.84	$C_{18}H_{37}$—N^+(—CH_3)(—CH_3)—$C_{18}H_{37}$
SB (dimethylstearyl benzylammonium)	37.9	4.01	$C_{18}H_{37}$—N^+(—CH_3)(—CH_3)—$CH_2C_6H_5$
HE (oreylbis(2-hydroxyethyl) methylammonium)	31.5	1.84	$H_2C(H_2C)HC=CH(H_2C)_7H_3C$—$N^+$(—$(CH_2CH_2O)xH$)(—$CH_3$)—$(CH_2CH_2)yH$

In this study, we plan to design an environmentally benign polymer composite that would have mechanical and thermal properties suitable for various end-use purposes. We add organophilic clay to the equimolar blend of PLLA and PDLA. Four types of organophilic clays are used (Table I). They are montmorillonite clays modified with trimethylstearyl ammonium (TM), dimethyloctadecyl ammonium (DO), dimethylstearyl benzylammonium (SB), and oreylbis(2-hydroxyethyl)methylammonium (HE). The effects of the clay type on the formation of stereocomplex-type crystal of PLA are investigated through the analysis of the crystalline structure, higher order structure, thermal properties, and mechanical properties of the PLLA/PDLA/clay blends.

EXPERIMENTAL

Materials

A commercial PLLA (Lacty, medical grade, $M_w = 2.2 \times 10^4$, $M_w/M_n = 1.96$) and a PDLA (PURAC, $M_w = 2.63 \times 10^4$, $M_w/M_n = 1.77$) were used in this study. Melting, crystallization, and glass transition temperatures of PLLA and PDLA as received were 177, 101, and 55°C, and 178, 109, and 54°C, respectively, as measured by differential scanning calorimetry (DSC). Four types of montmorillonite modified with quaternary ammonium salts were kindly supplied from Hojun, Co., Japan, and used as received. The chemical structure of the organic modifiers and the extent of inorganic component, which are provided by the supplier, are listed in Table I.

PLA/Clay Blends

Blends of PLLA, PDLA, and clay were prepared by solution-casting technique. Clay dispersion suspending 10 mg well-dried clay in 10 mL of methanol was obtained by sonication for 30

min at room temperature with a Misonix 3000 probe sonicator at 21 W. Pulse mode was used to prevent excessive increase in temperature. Immediately after the sonication, predetermined amount of the clay suspension were added to a solution containing 100 mg of PLLA and 100 mg of PDLA in 10 mL of chloroform, followed by further sonication for 30 min. The mixture was then cast on a glass Petri dish and kept in a desiccator over 2 days. Clear nanocomposite films with thickness ranging from 500 to 700 μm were obtained. The PLLA/PDLA/clay blends containing (100-#)/2 wt % PLLA, and (100-#)/2 wt % PDLA, and # wt % of clay are abbreviated as PLA/clay#. Annealing of the as-cast films was conducted at 170°C and 200°C in an oven for 2 h.

Analytical Procedures

Wide-angle X-ray diffraction (WAXD) patterns were obtained at room temperature using a nickel-filtered Cu Kα radiation with a wavelength of 0.1542 nm from a Rigaku RAD 2C sealed beam X-ray generator operating at 40 kV and 20 mA.

Thermal properties of the films were investigated with DSC (Perkin Elmer Pyris 1). A total of 5–10 mg of specimen was sealed in an aluminum pan. The DSC curve was recorded from 30 to 250°C at a rate of 10°C min^{-1} under a constant flow of nitrogen gas. Melting and crystallizing temperatures were determined from the maximum of the endothermic and exothermic peaks, respectively.

Thermal gravimetric analysis (TGA) was performed using Shimadzu TG in a N_2 atmosphere, by increasing the temperature from 30 to 500°C at a heating rate of 10°C min^{-1}.

Mechanical properties of the blend films were evaluated using a tensile testing machine (CATY-500BH: YONEKURA Ltd) at a
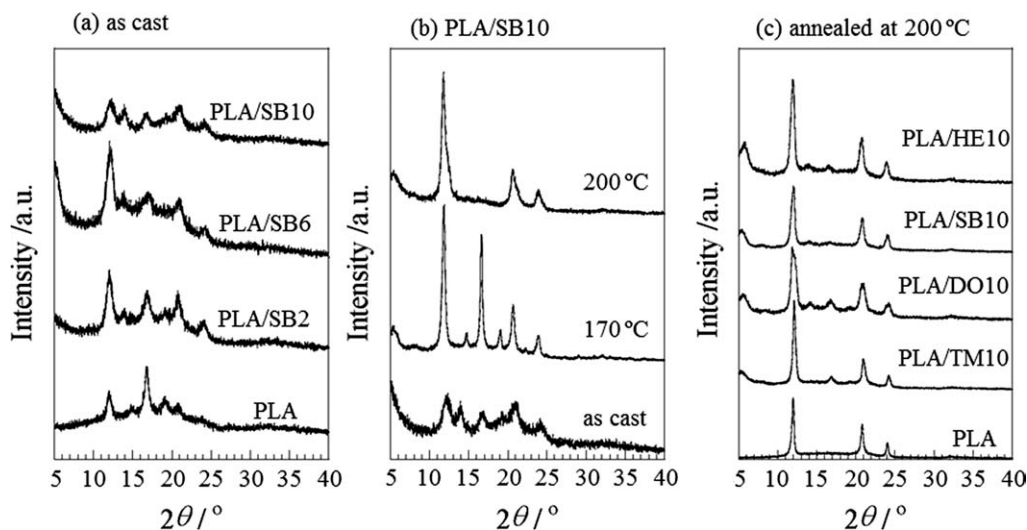
Figure 1. WAXD patterns of (a) as-cast PLA/SB blends containing 0–10 wt % SB, (b) PLA/SB10 as-cast and annealed at 170°C and 200°C, and (c) PLA/clay blends containing 10 wt % clays annealed at 200°C.

cross-head speed of 100 mm min^{-1} at a room temperature. A specimen gauge length of 20 mm was used. The results obtained were averaged over five pieces of each sample.

Transmission electron microscope (TEM) images of the samples were taken on a JEOL JEM-2000FX II transmission electron microscope at an acceleration voltage of 120 kV. Ultrathin (80 nm) sections were microtomed from the sample films in epoxy capsules which were prepared by curing at 70°C for 24 h in vacuum. A layer of carbon was deposited on each slice on a mesh 400 copper net.

RESULTS AND DISCUSSION

Crystalline Structure of PLA/Clay Blends

Two different crystal structures (α- and β-forms) have been proposed for PLLA, based on X-ray diffraction patterns and conformational energy analysis. The α-form of PLLA is in a pseudo-orthorhombic system with parameters of $a = 1.07$ nm, $b = 0.595$ nm, and c (fiber axis) $= 2.78$ nm.[40–42] Two chains with 10_3 helix conformation are contained in a unit cell. The β-form

appears in fibers drawn at higher temperature and/or with higher drawing ratios. An orthorhombic system is proposed for this structure ($a = 1.03$ nm, $b = 1.82$ nm, and c (fiber axis) $= 0.900$ nm), containing six chains with 3_1 helix conformation.[40] The crystal structure of the stereocomplex phase is different from these homocrystal structures.[43,44] The stereocomplex crystal system is triclinic ($P1$) with cell dimensions of $a = 0.916$ nm, $b = 0.916$ nm, c (fiber axis) $= 0.870$ nm, $\alpha = 109.2°$, $\beta = 109.2°$, and $\gamma = 109.8°$. Each of the PLA chains takes 3_1 helical conformation, which is extended slightly more than the 10_3 helix in the α-form homocrystal. PLLA and PDLA segments are packed laterally in a parallel fashion as a pair in the unit cell of the stereocomplex crystal.

The WAXD patterns of as-cast PLA/SB blends containing 0–10 wt % SB are shown in Figure 1(a). Neat PLA, i.e., equimolar blend of PLLA and PDLA showed reflections at $2\theta = 11.8°$, $17.0°$, $19.0°$, and $20.5°$. The reflections at $2\theta = 17.0°$ can be assigned to (110) and (200), and that at $2\theta = 19.0°$ to (203) and (204) of the α-form homocrystal. In the mean time, the
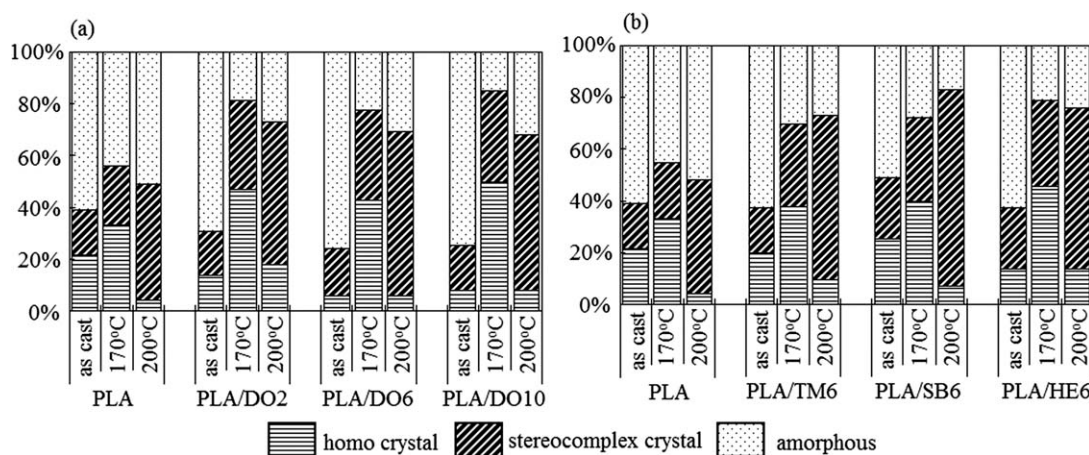

Figure 2. Homo- and stereocomplex crystallinities of (a) PLA/DO blends with 0–10 wt % DO and (b) PLA/clay blends containing 6 wt % clays.
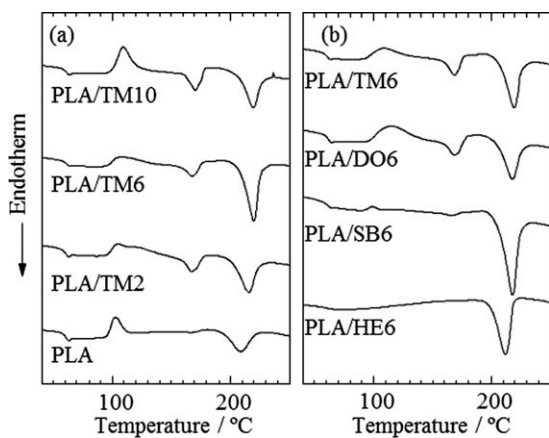
Figure 3. DSC heating traces of (a) as-cast PLA/TM blends containing 0–10 wt % TM and (b) as-cast PLA/clay blends with 6 wt % of clays.

reflection at $2\theta = 11.8°$ can be assigned to (100), (010), and (−110), and that at $2\theta = 20.5°$ to (110), (−120), and (−210) of the stereocomplex crystal. No reflections correspond to β-form homocrystal was observed for either neat PLA or the PLA/clay blends. By adding 2 or 6 wt % SB to PLA, the peak intensities of the stereocomplex crystal were enhanced. The addition of 10 wt % SB, on the other hand, reduced all the reflection peaks, indicating that the sample became amorphous-rich.

The WAXD patterns of as-cast and annealed PLA/SB10 is shown in Figure 1(b). Crystalline reflections of the annealed samples are larger than those of the as-cast sample. The annealing of PLA/SB10 at 170°C enhances both homo- and stereocomplex crystallization, whereas that at 200°C enlarges only the reflections of the stereocomplex crystal. Figure 1(c) shows the WAXD patterns of PLA/clay blends containing 10 wt % clays annealed at 200°C. The crystalline structure of these samples consists mainly of stereocomplex. Only small reflections are observed for

the homocrystal. This observation harmonize with the previous result showing enrichment of the stereocomplex crystals in the melt-processed PLA fiber.[24,25]

Peak separation of the WAXD patterns was performed to estimate the homo- and stereocomplex crystallinities. Figure 2(a) shows the homo- and stereocrystallinities of the as-cast and annealed PLA/DO samples. Both the homo- and stereocomplex crystallinities of the as-cast neat-PLA sample are about 20%. The addition of DO to the as-cast samples hardly effects the stereocomplex crystallization, whereas it gives a little tendency to reduce the homocrystallinity. Annealing at 170°C greatly enhances the homocrystallinity and slightly raises the stereocomplex crystallization at every DO contents. The effect of annealing is more emphasized in PLA/DO than in neat PLA. As a result, the total crystallinity, sum of the homo- and stereocomplex crystallinities, of the PLA/DO annealed at 170°C is extraordinarily high. By annealing at 200°C, the stereocomplex crystallinity in neat PLA and PLA/DO is significantly increased, whereas the homocrystallinity is drastically decreased.

The effects of other clays on the crystallinity were similar to those of DO. Figure 2(b) shows the homo- and stereocomplex crystallinities of the blend samples with 6 wt % of various clays. The difference among clay types is small compared with the effect of thermal treatment. The melting temperatures of homo- and stereocomplex crystals are about 180°C and 220°C, respectively. So, annealing at 170°C induced the enhancement of both homo- and stereocomplex crystallization, whereas annealing at 200°C resulted in the melting of homocrystal and the enhancement of stereocomplex crystallization.

Thermal Properties of the PLA/Clay Blends
Figure 3(a) shows the DSC thermograms of the as-cast PLA/TM with 0–10 wt % of TM. An exothermic peak was observed at a temperature around 110°C. This peak can be ascribed to the crystallization of PLA. Tsuji and Ikada[12] reported that the pure

Table II. Thermal Characteristics of Samples Obtained by DSC Measurements

Sample	T_g/°C[a]	$T_{m,H}$/°C[b]	$\Delta H_{m,H}$/Jg^{-1}[c]	$T_{m,S}$/°C[d]	$\Delta H_{m,S}$/Jg^{-1}[e,c]
PLA	46	171	2.0	205	10.2
PLA/TM2	57	172	11.5	215	16.6
PLA/TM6	58	171	7.1	215	23.0
PLA/TM10	53	173	11.2	214	18.1
PLA/DO2	51	173	12.2	215	19.0
PLA/DO6	57	171	13.2	216	20.4
PLA/DO/10	58	172	8.8	216	19.7
PLA/SB2	49	170	1.6	216	27.8
PLA/SB6	50	172	3.2	217	28.5
PLA/SB10	55	171	5.7	215	28.3
PLA/HE2	53	–	–	216	25.3
PLA/HE6	52	–	–	217	24.3
PLA/HE10	55	–	–	216	22.7

[a]Glass transition temperature at which half of the increase of heat capacity, [b]Melting temperature of homocrystal, [c]Heat of fusion of homocrystal, [d]Melting temperature of stereocomplex crystal, [e]Heat of fusion of stereocomplex crystal.
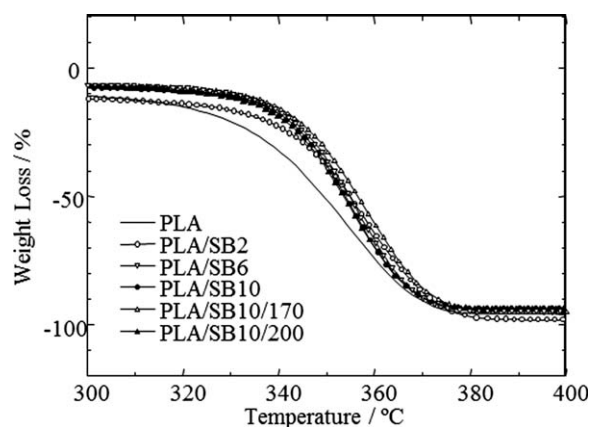
Figure 4. Thermogravimetric traces of as-cast PLA/SB blends containing 0–10 wt % SB and PLA/SB10 annealed at 170°C and 200°C.

PLLA or PDLA show a homocrystallization peak around 90°C, whereas PLLA/PDLA equimolar blend show stereocomplex crystallization around 70°C. It is, however, not possible at this moment to distinguish whether the exothermic peak around 110°C of the PLA/TM blends is the homocrystallization or the stereocomplex crystallization.

In the thermogram of the neat PLA, only the melting peak of the stereocomplex crystal was observed at around 210°C, whereas in the thermograms of PLA/TM blends, the melting peak of the α-form homocrystal was also observed at around 170°C. The peak area of the homocrystal melting endothermic peak at around 170°C increased with adding TM. As shown in Figure 2(b), the as-cast neat PLA sample surely contained the homocrystal. The absence of the melting peak of the homocrystal in the thermograms suggests that the homocrystal was rearranged to the stereocomplex crystal during the DSC heating scan of this sample. In the PLA/TM samples, this rearrangement of the crystals might be retarded by the existence of TM.

Figure 3(b) shows the DSC thermograms of PLA/clay with 6 wt % of clays. Similar to the neat PLA, the homocrystal melting peak was absent in the thermograms of PLA/SB and PLA/HE, indicating that the homocrystal was rapidly rearranged to the stereocomplex crystal during the DSC heating. On the other hand, PLA/DO had both the endothermic peaks at around

170°C and 210°C like PLA/TM. The existence of DO also retards the rearrangement of the crystals like TM. The organic parts of the SB and HE clays, respectively, contain of bulky benzyl and hydrophilic hydroxyl units, whereas that of TM and DO consists of rather simple linear alkyl groups. This structural difference may affect the compatibility of the montmorillonite clay to PLA. TM and DO may be more intimately mixed with PLA. It should be noted that when the 2nd heating process was performed after melting and quenching the PLA/clay samples, DSC traces show only melting of the stereocomplex crystals in all the samples (data not shown).

Table II shows glass transition temperature, melting temperatures of homo- and stereocomplex crystals, and heat of fusion of the samples. The glass transition temperature of PLA was increased about 4–14°C by adding clay. Melting temperature of the stereocomplex crystal becomes higher by adding clay. These results indicate that the addition of clay induces well-ordered crystallization PLA while it reduces the mobility of molecular chains.

Figure 4 shows the thermogravimetric traces of PLA and PLA/SB. The degradation of the as-cast neat PLA starts at about 300°C and ends at about 380°C. By adding SB, the onset temperature of weight loss increases to about 340°C, whereas the end temperature remains unchanged. The content of SB and thermal history (annealing at 170°C and 200°C) does not affect the degradation profile. We have confirmed that the other clays gave similar effects on the decomposition profile of PLA. These results are in line with other biodegradable aliphatic polyester nanocomposites.[45] The change in the degradation temperature in PLA/clay is, however, quite small compared with that in polypropylene nanocomposites.

Mechanical Properties of PLA/Clay Blends

Figure 5(a–c) shows the mechanical properties of the as-cast and annealed PLA/DO samples as a function of clay content. The addition of clay and annealing hardly affect Young's modulus of PLA. The tensile strength of the neat PLA was increased by annealing at 170°C, whereas decreased by annealing at 200°C, because of the slight thermal degradation. This result indicates that the homocrystals strengthen PLA, whereas stereocomplex crystals deteriorate it. On the other hand, annealing of
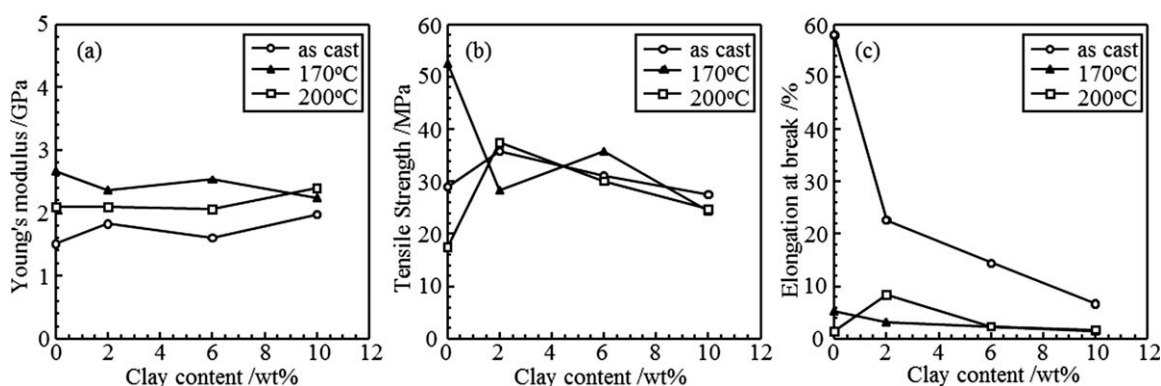

Figure 5. (a) Tensile modulus, (b) strength, and (c) elongation at break of PLA/SB films as a function of clay contents.
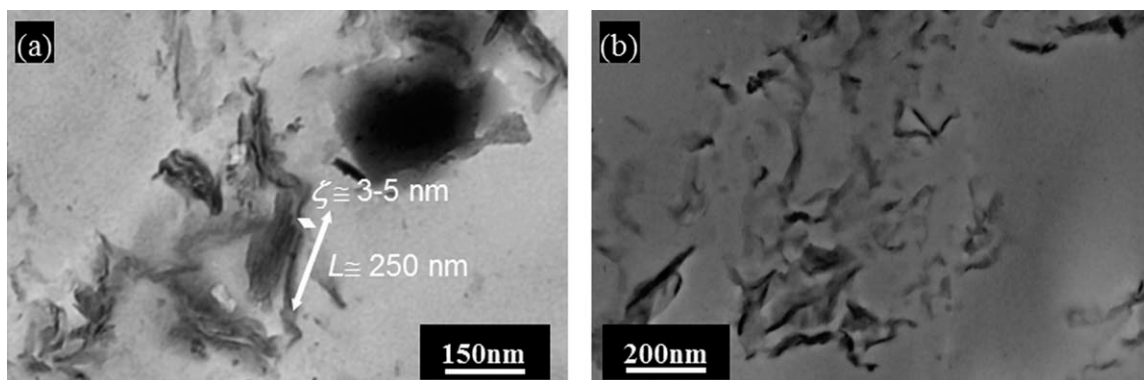
Figure 6. TEM micrographs of PLA/SB6 annealed at (a) 170°C and (b) 200°C.

PLA/clay at 170°C hardly raise the tensile strength, suggesting that the interaction between the homocrystal and the clay deteriorates tensile strength. The elongation at break of the neat PLA was greatly decreased by annealing. This means that the sample with lower crystallinity has higher elongation at break. However, the as-cast PLA/DO samples, which have similar crystallinity to the as-cast neat PLA, show lower elongation at break. So the clays that have been trapped in the amorphous region negatively affect the tensibility. In short, though annealing treatment changes the mechanical properties of neat PLA, this effect is suppressed by the addition of clay. All the other clays show the same tendencies as DO.

Higher Order Structure of PLA/Clay Blends

The higher order structure of the polymer/clay blends has typically been elucidated using TEM and WAXD. WAXD allows a direct observation of the intercalation of the polymer chains into the silicate galleries. TEM offers a qualitative understanding of the internal structure of the PLA/clay in the nanometer scale through direct visualization. Figure 6 shows typical TEM bright images of PLA/SB6 annealed at 170°C and 200°C, in which dark entities are the cross section of intercalated silicate layers. The aggregation of layers was observed in the sample annealed at 170°C. Typical silicate layers of montmorillonite have a thickness of about 1 nm and a length of about 150 nm. In the sample annealed at 170°C, some of the stacked silicate layers reach a length (L_{clay}) of about 250 nm owing to the hydroxylated edge–edge interaction of silicate layers. The thickness of each layer in the stack was about 3–5 nm (ζ_{clay}) from the TEM photographs. The stacks of layers are randomly distributed in the PLA matrix. On the other hand, the exfoliation of clay was observed in the sample annealed at 200°C.

Figure 7(a) shows the WAXD patterns in the clay reflection area ($2\theta = 1$–$10°$) of as-cast PLA/SB with 2–10% of SB. The pattern of neat SB is also given. Neat SB shows reflections at 3.76 nm and 1.96 nm, which were assigned to the (001) and (002) planes of the stacked silicate layers, respectively. In PLA/SB6, a sharp peak at $2\theta = 2.8°$ (3.15 nm) and a small broad peak at $2\theta = 5.2°$ (1.70 nm), correspond to the (001) and (002) planes of the intercalated silicate layers, respectively. The existence of a sharp Braggs peak at $2\theta = 2.8°$ (3.15 nm) shows that the clay still remains in an ordered stacking state after blending with PLA

although the interlayer spacing decreased compared with that of the clay powder. Therefore, this peak is assigned to the clay that is aggregated and stacked by the clay itself. Some level of clay aggregation was kept in the polymer matrix because of the expulsion of inorganic additive in the organic matrix. The peak intensity and lattice spacing increased with increasing clay content. In the case of PLA/SB2, the clay reflection was not detected, indicating that the clay layers are delaminated.

Figure 7(b) shows the WAXD patterns of PLA/SB6 annealed at different temperatures. Annealing at 170°C enhances the crystallization of clay, indicated by the sharper reflections of (001) and (002). The clay spacing of this sample is smaller than that of neat SB, indicating the exfoliation occurs with the polymer chains in the silicate layers. The sample annealed at 200°C shows the larger spacing of clay than neat SB and PLA/SB6 annealed at 170°C. The reflections are large and wide, indicating the occurrence of clay disordering during annealing.

Comparison Between Other Clay Blends

There are many reports concerning about the preparation of PLLA/clay nanocomposites by melt blending.[32–37] The intercalation of PLLA polymer chains into the silicate layers were demonstrated. The improvement of thermal stability up to 9°C, mechanical properties such as storage modulus, flexural modulus,
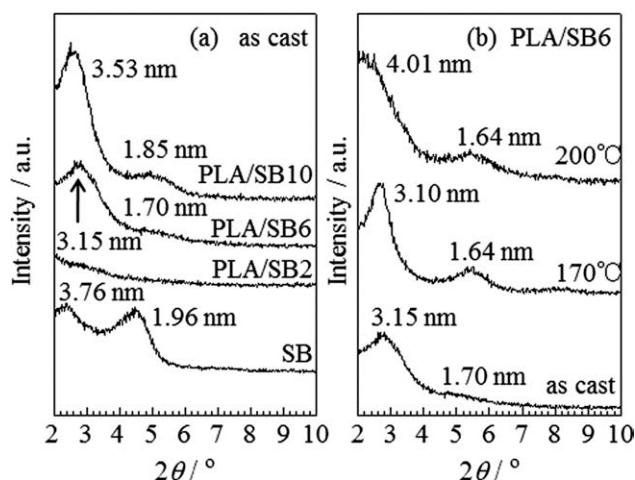

Figure 7. WAXD patterns of SB and as-cast and annealed PLA/SB6.

flexural strength, and gas barrier property has been observed. This achievement might be because of the intercalation and exfoliation between PLLA and silicate layers. Intercalation readily occurred between PLLA and silicates during melt blending.

Ogata et al. have reported about some properties of PLLA/clay blends prepared by solvent-casting. Young's modulus increased from 1.3 to 2.3 GPa with the addition of up to 10 wt % of clay.

In spite of so many reports on the PLLA/clay blends, this might be the first report concerning the layered silicate nanocomposites of PLLA/PDLA stereocomplex. Although mechanical properties of the solution-casting blend of PLLA/PDLA/clay are slightly improved, thermal stability is hardly changed. PLA is exfoliated in silicate layers. The interaction between stereocomplex PLA and silicate layers is hardly improved, which do not lead significant change of mechanical properties. If the intercalation of PLA to silicate layers were prepared by melt blending or extrusion, we hope that the thermal stabilities and mechanical properties will be improved. This assignment will be reported in near future.

CONCLUSIONS

PLLA/PDLA/organo-clay blends have been prepared by solution casting, followed by annealing. WAXD and TEM analysis showed that the silicate layers of the clay were slightly stacked but intercalated and distributed in the PLA-matrix. Therefore, it has been represented that organo-clay can be dispersed in PLLA/PDLA matrix simply by the solution-casting method while keeping the stereocomplex crystallization of the PLA matrix. The annealing at 170°C enhances both the homo- and stereocomplex crystallization, whereas that at 200°C greatly enhances only the stereocomplexation. The effect of annealing was emphasized by the addition of clay. Thermal stabilities and mechanical properties were also slightly improved by the addition of clay. Although annealing treatment changes the mechanical properties of neat PLA, this annealing effect is suppressed by the addition of clay.

REFERENCES

1. Vert, M.; Christel, P.; Chabot, F.; Leray, J. In Macromolecular Materials; Hasting, G. W., Ducheyne, P., Eds.; CRS Press: Florida, **1984;** pp 119–142.

2. Ikada, Y.; Jamshidi, K.; Tsuji, H.; Hyon, S. H. *Macromolecules* **1987,** *20*, 904.

3. Tsuji, H.; Horii, F.; Hyon, S. H.; Ikada, Y. *Macromolecules* **1991,** *24*, 2719.

4. Tsuji, H.; Hyon, S. H.; Ikada, Y. *Macromolecules* **1991,** *24*, 5651.

5. Tsuji, H.; Hyon, S. H.; Ikada, Y. *Macromolecules* **1991,** *24*, 5657.

6. Tsuji, H.; Hyon, S. H.; Ikada, Y. *Macromolecules* **1992,** *25*, 2940.

7. Tsuji, H.; Ikada, Y. *Macromolecules* **1992,** *25*, 5719.

8. Tsuji, H.; Horii, F.; Nakagawa, M.; Ikada, Y.; Odani, H.; Kitamaru, R. *Macromolecules* **1992,** *25*, 4114.

9. Tsuji, H.; Ikada, Y. *Macromolecules* **1993,** *26*, 6918.

10. Brochu, S.; Prud'homme, R. E.; Barakat, I.; Jérôme, R. *Macromolecules* **1995,** *28*, 5230.

11. Brizzolara, D.; Cantow, H. J.; Diederichs, K.; Keller, E.; Domb, A. J. *Macromolecules* **1996,** *29*, 191.

12. Tsuji, H.; Ikada, Y. *Macromol. Chem. Phys.* **1996,** *197*, 3483.

13. Cartier, L.; Okihara, T.; Lotz, B. *Macromolecules* **1997,** *30*, 6313.

14. Kister, G.; Cassanas, G.; Vert, M. *Polymer* **1998,** *39*, 267.

15. Tsuji, H.; Ikada, Y. *Polymer* **1999,** *40*, 6699.

16. Tsuji, H. *Polymer* **2000,** *41*, 3621.

17. Serizawa, T.; Yamashita, H.; Fujiwara, T.; Kimura, Y.; Akashi, M. *Macromolecules* **2001,** *34*, 1996.

18. Bourque, H.; Laurin, I.; Pézolet, M.; Klass, J. M.; Lennox, R. B.; Brown, G. R. *Langmuir* **2001,** *17*, 5842.

19. Serizawa, T.; Arikawa, Y.; Hamada, K.; Yamashita, H.; Fujiwara, T.; Kimura, Y.; Akashi, M. *Macromolecules* **2003,** *36*, 1762.

20. Urayama, H.; Moon, S. I.; Kimura, Y. *Macromol. Mater. Eng.* **2003,** *288*, 137.

21. Tsuji, H.; Tezuka, Y. *Biomacromolecules* **2004,** *5*, 1181.

22. Zhang, J.; Sato, H.; Tsuji, H.; Noda, I.; Ozaki, Y. *Macromolecules* **2005,** *38*, 1822.

23. Tsuji, H. *Macromol. Biosci.* **2005,** *5*, 569.

24. Furuhashi, Y.; Kimura, Y.; Yamane, H. *J. Polym. Sci. Part B: Polym. Phys.* **2007,** *45*, 218.

25. Furuhashi, Y.; Kimura, Y.; Yoshie, N.; Yamane, H. *Polymer* **2006,** *47*, 5965.

26. Furuhashi, Y.; Yoshie, N. *Polymer Int.* **2012,** *61*, 301.

27. Serizawa, S.; Inoue, K.; Iji, M. *J. Appl. Polym. Sci.* **2006,** *100*, 618.

28. Ganster, J.; Fink, H. P. *Cellulose* **2006,** *13*, 271.

29. Kasuga, T.; Ota, Y.; Nogami, M.; Abe, Y. *Biomaterials* **2001,** *22*, 19.

30. Okamoto, M. Handbook of Biodegradable Polymeric Materials and Their Applications; American Scientific Publishers: Stevenson Ranch, CA, **2005;** pp 1–45.

31. Ogata, N.; Jimenez, G.; Kawai, H.; Ogihara, T. *J. Polym. Sci. Part B: Polym. Phys.* **1997,** *35*, 389.

32. Ray, S. S.; Maiti, P.; Okamoto, M.; Yamada, K.; Ueda, K. *Macromolecules* **2002,** *35*, 3104.

33. Pluta, M.; Galeski, A.; Alexandre, M.; Paul, M.-A.; Dubois, P. *J. Appl. Polym. Sci.* **2002,** *86*, 1497.

34. Ray, S. S.; Yamada, K.; Okamoto, M.; Ueda, K. *Polymer* **2003,** *44*, 857.

35. Chang, J.-H.; An, Y. U.; Cho, D.; Giannelis, E. P. *Polymer* **2003,** *44*, 3715.

36. Paul, M.-A.; Alexandre, M.; Degee, P.; Calberg, C.; Jerome, R.; Dubois, P. *Macromol. Rapid Commun.* **2003,** *24*, 561.

37. Paul, M.-A.; Alexandre, M.; Degee, P.; Henrist, C.; Rulmont, A.; Dubois, P. *Polymer* **2003,** *44*, 443.

38. Krikorian, V.; Pochan, D. J. *Macromolecules* **2004,** *37*, 6480.

39. Krikorian, B.; Pochan, D. J. *Macromolecules* **2005,** *38*, 6520.

40. De Santis, P.; Kovacs, A. J. *Biopolymers* **1968,** *6*, 299.

41. Hoogsteen, W.; Postema, A. R.; Pennings, A. J.; ten Brinke, G.; Zugenmaier, P. *Macromolecules* **1990,** *23*, 634.

42. Kobayashi, J.; Asahi, T.; Ichiki, M.; Oikawa, A.; Suzuki, H.; Watanabe, T.; Fukada, E.; Shikinami, Y. *J. Appl. Phys.* **1995,** *77*, 2957.

43. Okihara, T.; Kawaguchi, A.; Tsuji, H.; Hyon, S. H.; Ikada, Y.; Katayama, K. *Bull. Inst. Chem. Res. Kyoto Univ.* **1988,** *66*, 271.

44. Okihara, T.; Tsuji, M.; Kawaguchi, A.; Katayama, K. *J. Macromol. Sci. Phys.* **1991,** *B30*, 119.

45. Lim, S. T.; Hyun, Y. H.; Choi, H. J. *Chem. Mater.* **2002,** *14*, 1839.